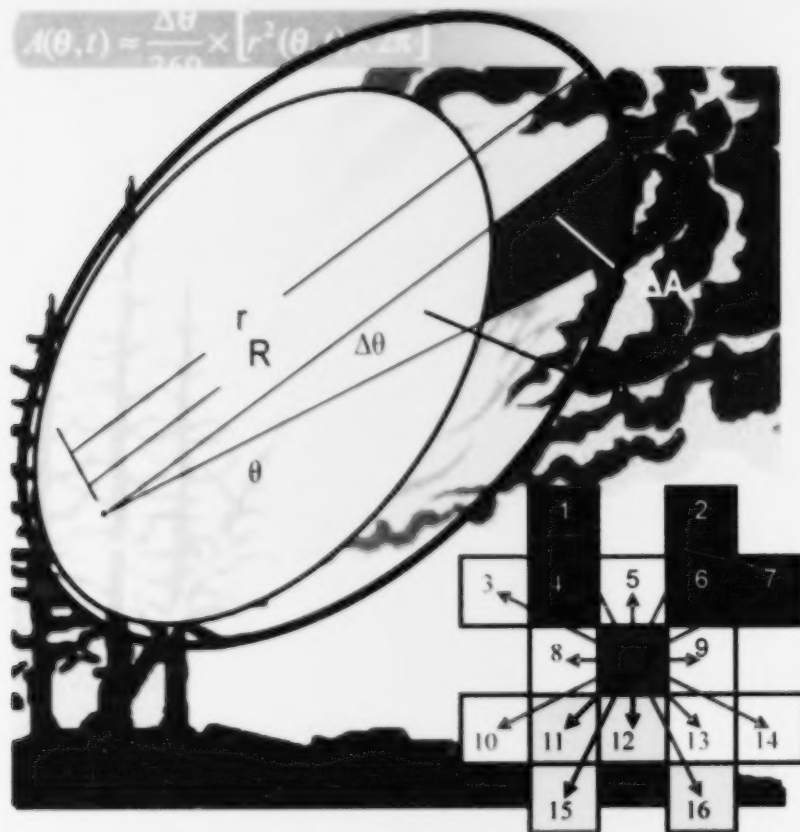# A study of simulation errors caused by algorithms of forest fire growth models

Ontario

A study of simulation errors caused by algorithms of forest fire growth models

Wenbin Cui and Ajith H. Perera

2008

Cette publication hautement spécialisée *A study of simulation errors caused by algorithms of forest fire growth models* n'est disponible qu'en anglais en vertu du Règlement 411/97, qui en exempte l'application de la Loi sur les services en français. Pour obtenir de l'aide en français, veuillez communiquer avec le ministère des Richesses naturelles au information.ofri@ontario.ca.

This paper contains recycled materials.

Abstract

Forest fire growth models (FGMs) simulate fire spread over spatially heterogeneous forest landscapes and over long periods with changing weather conditions. It is challenging to validate these models. The simulation errors of a FGM arise from three major sources: (1) the availability and quality of input data, (2) the theoretical basis of the fire behaviour model, and (3) the fire growth algorithm. Errors caused by the algorithm are an indicator of the algorithm performance of FGMs. We studied the errors by assessing the algorithm performance of three FGMs: the FGM in BFOLDS (Boreal Forest Landscape Dynamics Simulator), Prometheus, and Wildfire. We examined the shapes and sizes of simulated fire perimeters compared to those predicted by the Forest Fire Behaviour Prediction (FBP) system under four spatial resolutions, five wind directions, and two spatial configurations of fuel type, keeping weather, topography, and other input data constant. Two new indices were used for error analysis. Our results suggest: (a) large fire simulation errors were caused by the fire growth algorithms of all three FGMs; (b) finer spatial resolutions did not necessarily produce more accurate predictions for BFOLDS and Prometheus; (c) simulation errors occurred mainly in the direction of head fire for all three models; and (d) the event-driven, continuous time advancing algorithm helps reduce error accumulation.

Résumé

Les modèles de développement des feux de forêt (MDFF) simulent la propagation des incendies sur les paysages forestiers spatialement hétérogènes et sur de longues périodes, en fonction des conditions météorologiques changeantes. La validation de ces modèles est problématique. Les erreurs de simulation d'un MDFF sont dues à trois principaux facteurs : (1) la disponibilité et la qualité des données d'entrée, (2) la base théorique du modèle de comportement de l'incendie et (3) l'algorithme de propagation des feux. Les erreurs dues à l'algorithme sont un indicateur de la performance algorithmique des MDFF. Nous avons examiné les erreurs en évaluant la performance algorithmique de trois MDFF : ceux qui ont été utilisés dans BFOLDS (simulateur de la dynamique des paysages de la forêt boréale), Prometheus et Wildfire. Nous avons examiné les formes et les dimensions des périmètres d'incendies simulés par rapport à celles qui avaient été prévues par la méthode de prévision du comportement des incendies de forêt (PCIF) selon quatre résolutions spatiales, cinq directions du vent et deux configurations spatiales du type de combustible, en maintenant constantes les conditions météorologiques, la topographie et les autres données d'entrée. Deux nouveaux indices ont été utilisés pour l'analyse des erreurs. Les résultats que nous avons obtenus laissent supposer que : a) les grosses erreurs de simulation d'incendies étaient dues aux algorithmes de développement des feux des trois MDFF; b) les résolutions spatiales plus détaillées ne donnent pas nécessairement des prévisions plus exactes pour BFOLDS et Prometheus; c) les erreurs de simulation concernaient surtout la direction du feu poussé par le vent, pour les trois modèles; et d) l'algorithme d'avance continue dans le temps, dirigé par les événements, aide à réduire l'accumulation d'erreurs.

Acknowledgements

Contents

Introduction

Forest fire growth models (FGM) are increasingly used not only by fire researchers for academic purposes, but also by forest and fire managers to support management decisions at various spatial and temporal scales (Hargrove *et al.* 2000, Finney 2001, Sánchez-Guisández *et al.* 2002, Anderson *et al.* 2007). In forest fire management, FGMs are used in both operations and planning (Finney 2001, Sánchez-Guisández *et al.* 2002, Opperman *et al.* 2006). FGMs are also used to design and evaluate fuel treatment strategies (Finney 2001, Sánchez-Guisández *et al.* 2007) and have been integrated into wildland urban interface (WUI) management decision support systems (Sánchez-Guisández *et al.* 2007). When used at landscape or regional scale and in long-term forest and fire management planning, FGMs are often embedded in larger models (Hargrove *et al.* 2000), for example as a component of a forest fire regime model that simulates both fire and succession processes (Perera *et al.* 2004).

FGMs involve spatially and temporally explicit modelling of forest fire spread over large spatially heterogeneous (vegetation and topography) forest landscapes over durations of days or even months under changing weather conditions. Hence, it is not only difficult to build FGMs to precisely predict fire growth, but also difficult to validate the models (Trunfio 2004). A typical method of validating FGMs is to graphically compare predicted perimeters to the corresponding perimeters of the actual fires they simulate (Berjak and Hearne 2002, Trunfio 2004, CWFGM Project Steering Committee 2006, Opperman *et al.* 2006, Anderson *et al.* 2007). One limitation with this method is that it is only a visual and qualitative rather than quantitative evaluation of errors. Also it is not spatially explicit and cannot be used to distinguish causes of errors or to indicate to what degree an error results from a given factor.

Errors associated with FGM simulations come primarily from three main sources: input data used in simulations, fire behaviour model used in the FGM, and the specific algorithms that constitute the FGM. FGMs require spatially explicit data for fuel and topography (elevation, slope, and aspect), and spatio-temporal data for weather conditions, which mainly include temperature, humidity, rainfall, wind speed and direction,

and possibly other weather variables depending on the specific models. These data may be incomplete, of low quality, or too coarse in spatial (e.g., weather, fuel, and topography) and temporal resolution (e.g., weather). The second source of error arises from the fire behaviour model on which the FGM is based. Regardless of the type of fire behaviour model, which may be semi-physical, such as Rothermel's (1972), or empirical, such as the Canadian Forest Fire Behaviour Prediction (FBP) system (Forestry Canada Fire Danger Group 1992), their design and approach have inherent limitations or errors. These fire behaviour models may use, for example, simplistic assumptions for physical or semi-physical models (Rothermel 1972) or highly variable data to develop empirical models (Forestry Canada Fire Danger Group 1992). The third source of error involves the fire growth algorithm used to extend the fire behaviour model to a FGM.

Even when the input data are of high quality, a FGM can still have simulation errors when compared to the theoretical predictions of the fire behaviour model it uses. These errors may confound and accumulate during simulations as shown in Figure 1. In the end, the errors in simulations may not only have multiplied, but their sources may also be indistinguishable. Most, if not all, previous studies on FGMS (e.g., Berjak and Hearne 2002, Trunfio 2004, Opperman *et al.* 2006) have not isolated sources of simulation error.
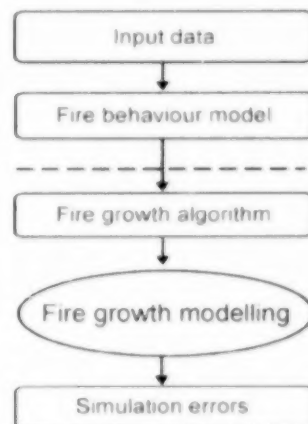

Figure 1. *Error propagation occurs throughout forest fire growth modelling. Sources of error are the input data, the fire behaviour model, and the fire growth algorithm.*

Identifying the exact contribution of these sources of errors is important to evaluate and validate FGMs. However, the most important reason for detecting, quantifying, and isolating these sources of errors is that it is essential for continuous improvement to FGMs – regardless of whether the fire behaviour model, the coding, or the data usage are the target of improvements. Identifying the specific errors associated with algorithms provides the most efficient and expedient means for fire growth modellers to improve FGMs in the short term, whereas improving input data quality and availability and advancing the fire behaviour knowledge are longer-term and costlier endeavours.

In this context, we conducted a study to isolate and detect errors that stem from the FGM algorithm by separating those from the errors that arise from input data and the fire behaviour model. To control the errors associated with the fire behaviour model, we used three FGMs that are based on the same parent fire behaviour model – the Canadian FBP system. To control the data errors, we used the same input data – identical in type as well as spatio-temporal resolution. Thus, we could isolate, detect, and quantify the errors that arise from algorithms associated with the FGMs. We expect that this knowledge will aid algorithm improvements of the three FGMs specifically, and other FGMs in general. Our specific objectives in this study were (1) to examine the algorithm performance of the three FGMs compared to the corresponding theoretical calculations from the FBP system under controlled conditions of input data (spatial resolutions, wind directions, and spatial configuration of fuel types), (2) to analyze errors specific to certain FGM algorithms, and (3) to explore ways to improve the FGM algorithms based on our findings. To accomplish these objectives, we introduced new indices to measure and compare size and shape errors of predicted forest fire perimeters.

Methods

Three forest fire growth models

We selected three FGMs for comparison, mainly based on algorithm characteristics and to a lesser degree on their frequency and scope of use. The three FGMs are the FGM in BFOLDS (Boreal Forest Landscape Dynamics Simulator), Prometheus, and Wildfire. BFOLDS is a forest fire regime model that simulates forest fires and succession over large boreal forest landscapes (millions of hectares) and long periods (hundreds of years). It was developed by the Forest Landscape Ecology Program at the Ontario Forest Research Institute and has been used as a decision support tool in the formulation of forest management policy in the province of Ontario, Canada (Perera et al. 2003, 2004). We refer to the FGM in BFOLDS simply as BFOLDS in this report. Prometheus development was lead by Alberta Sustainable Resource Development and endorsed by the Canadian Interagency Forest Fire Centre (CIFFC) and its members (CWFGM Project Steering Committee 2006). It is widely used in much of Canada in operations and research. Wildfire was developed by the Canadian Forest Service (Todd 1999) and has been used in some research models and wildland-urban interface decision support systems (Sánchez-Guisández et al. 2002).

All three FGMs are deterministic (Todd 1999, CWFGM Project Steering Committee 2006) and are based on the FBP system (Forestry Canada Fire Danger Group 1992), the Canadian Forest Fire Weather Index (FWI) system (Van Wagner and Pickett 1985), and use Huygens' Principle of wave propagation with the simple ellipse as the underlying template to shape fire growth (Todd 1999, CWFGM Project Steering Committee 2006). The models also use similar inputs both in content and format. For example, they all use raster-based ASCII format for the spatial inputs of FBP fuel type, slope, and aspect. In this format, a landscape property is represented by a matrix of squares (called rasters) with the raster as the smallest unit. Each unit can have only one value for each property. For example, the spatial configuration of FBP fuel types can be defined by assigning a fuel type value to each raster.

The present version of BFOLDS uses the fuel type of the source raster to calculate the rate of spread (ROS) for each spread direction, regardless of the fuel types of neighbouring rasters (Figure 2). Note that the ROS in a direction is zero if any of the cells on that path are not burnable, either because they burned earlier or are, for example, rock or water. BFOLDS advances time continuously based on an event-driven algorithm. The fire in an ignited raster (source) will spread to its 16 neighbour rasters if they are burnable (i.e., contain a burnable fuel type). If the neighbour raster (target) is burnable, then the time that the fire reaches the target raster is calculated as:

$$time = distance / ROS \qquad (1)$$

where ROS is the rate of spread from the source raster to each target raster calculated based on the FBP system equations (Forestry Canada Fire Danger Group 1992) and the elliptical model (Catchpole et al. 1982). When the time is reached, the target raster will burn if it has not yet been burned by fire spread from other source rasters. This event-driven algorithm avoids the accumulated simulation errors caused by fixed, discrete time steps. It also enables the simultaneous simulation of multiple fires on a landscape of tens of millions of hectares over the whole fire season.
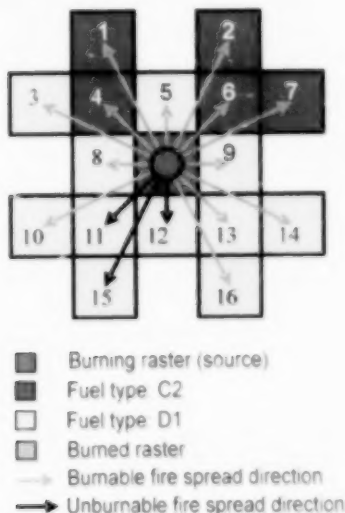

Figure 2. Schematic figure of the 16-direction fire spread algorithm in BFOLDS.

Prometheus and Wildfire grow fires by discrete time steps and only calculate and project the fire perimeters at each time step. Then, based on the new perimeter, they project a perimeter for the next time step. The value of a time step is 10 minutes for Wildfire (Todd 2001, Canadian Forest Service, pers. comm.). The value is adjustable for Prometheus but a value of 10 minutes was used in this study.

These FGMs differ mainly in their fire growth algorithms. The major differences include: (1) Prometheus uses a vector-based fire growth algorithm (Richards 1990, Richards and Bryce 1995) while BFOLDS and Wildfire use raster-based fire growth algorithms; (2) BFOLDS uses a 16-direction fire spread algorithm and Wildfire uses an eight-direction fire spread algorithm; and (3) BFOLDS advances time continuously based on an event-driven algorithm while Prometheus and Wildfire advance time in discrete steps (Todd 1999, CWFGM Project Steering Committee 2006). Other minor algorithm differences that mainly affect their implementation are outside the intent of this study.

Simulation conditions and test variables

To compare the FGMs, base conditions were kept constant as follows: the size of the study was 60 km by 60 km (360,000 ha) with a level surface (slope is 0). Each simulated fire lasted 15 hours and a single constant weather scenario was used: temperature was 27.6°C, relative humidity was 18%, wind speed was 16.0 km·h⁻¹, 24-hour cumulative rainfall was 0 mm, and FFMC, DMC, BUI[1] were 95, 42, and 42, respectively. The values were kept constant over the 15-hour period for all the simulation runs.

[1] FFMC, DMC, and BUI are indices of Canadian FWI system. FFMC (fine fuel moisture code) is a numeric rating of the moisture content of litter and other cured fine fuels. This code is an indicator of the relative ease of ignition and the flammability of fine fuel. DMC (duff moisture code) is a numeric rating of the average moisture content of loosely compacted organic layers of moderate depth. This code indicates fuel consumption in moderate duff layers and medium-size woody material. DC (drought code) is a numeric rating of the average moisture content of deep, compact organic layers and large woody material. This code is a useful indicator of seasonal drought effects on forest fuels and the amount of smouldering in deep duff layers and large logs. BUI (build up index) is a numeric rating of the total amount of fuel available for combustion. It combines the DMC and the DC (Van Wagner and Pickett 1985)

The test variables were (1) spatial configuration of fuel types, (2) spatial resolution of the landscape inputs (FBP fuel type), and (3) wind direction. Two spatial configurations of fuel types were used. The first, RM, was a randomly distributed configuration of two kinds of raster cells, black spruce and leafless aspen, defined as C2 and D1, respectively, in the FBP system (Forestry Canada Fire Danger Group 1992). Each fuel type made up 50% of the total number of rasters. The second, M1, was one type of raster cell: a boreal mixedwood of black spruce (50%) and leafless aspen (50%) referred to as M1_%50 in the FBP system, but for simplicity, we use M1 in this report.

Four spatial resolutions were studied. The raster sizes were 4.00, 1.00, 0.36, and 0.09 ha (corresponding sides of 200, 100, 60, and 30 m), respectively, where 0.09 ha is the smallest raster size that Wildfire can support and 4.00 ha is large for a landscape process. Five wind directions were tested: 0°, 22.5°, 45°, 67.5°, and 90° based on the direction system used in the FBP system in which the 0° angle is north-south and increases clockwise. Thus, wind directions are equivalent to 270°, 247.5°, 225°, 202.5°, and 180° in the mathematical direction system in which the 0° angle is west-east and increases counter clockwise. We used the mathematical direction system in this paper. (Directions 247.5° and 202.5° were not used for Wildfire, because it supports only eight wind directions: 0°, 45°, 90°, 135°, 180°, 225°, 270°, and 315°). The tested wind directions were all in the same quadrant and no other directions were used due to the symmetry (spatial configuration of M1) or approximate symmetry of the landscape (spatial configuration of RM).

There are certainly other factors that affect the FGM prediction accuracy, such as wind speed, other weather variables, and topography. We did not intend to study all possible factors. Here we selected three factors that we deemed most affect the fire growth algorithm, in contrast to those that may most affect fire behaviour but not matter as much to fire growth algorithm performance. For example, wind direction does not affect fire behaviour in uniform fuels but does affect the accuracy of fire growth.

The perimeters predicted in the simulations were then compared to the corresponding perimeters predicted by the FBP system.

FBP predictions

Based on the FBP system equations (Forestry Canada Fire Danger Group 1992) and the elliptical fire growth model (Catchpole et al. 1982) used by all three models compared, we simulated fire growth for the same five wind directions (180°, 202.5°, 225°, 247.5°, and 270°) in the uniform fuel type M1. These predictions were used as the basis for comparison with predictions from each FGM using the same wind directions under different spatial resolutions and fuel configurations as described above.

The assumption for the comparisons was that both spatial configurations of M1 and RM fuel type had the same fuel type composition (50% black spruce and 50% leafless aspen) and at infinitely small raster size RM would become M1. Thus, in theory, all predictions by the three models for the two fuel configurations should be similar to those predicted by the FBP system (on which the three FGMs are based) using the uniform fuel type, M1. And, the finer the resolution, the more similar they should be.

Fire simulation error index

We compared not only the sizes (aspatial) but also the shapes of the predicted fires by introducing two new indices, one for overall fire simulation error and one for fire simulation error in size by fire spread direction.

For this study, we used a method for the spatial analysis of two-dimensional fire growth simulation errors. It is similar to Fujioka's (2002) method in that it describes fire simulation errors in a spatially explicit manner. The measure, which we term fire *Simulation Error Index (SEI)* can be used to gauge the error in fire growth simulations. The fire perimeters were represented using the polar coordinate system with the ignition point as the origin. We let $r(\theta, t)$ represent the actual fire perimeter at time t and $R(\theta, t)$ represent the corresponding simulated perimeter predicted by a FGM at time t. *SEI* was defined as:

$$SEI(\theta, t) = \Delta A(\theta, t) = a(\theta, t) - A(\theta, t) \qquad (2)$$

where A and a are the area of simulated fire size and the actual fire area, respectively, within an increment of angle $\Delta\theta$ at angle θ, and ΔA is the area difference between a and A (Figure 3).
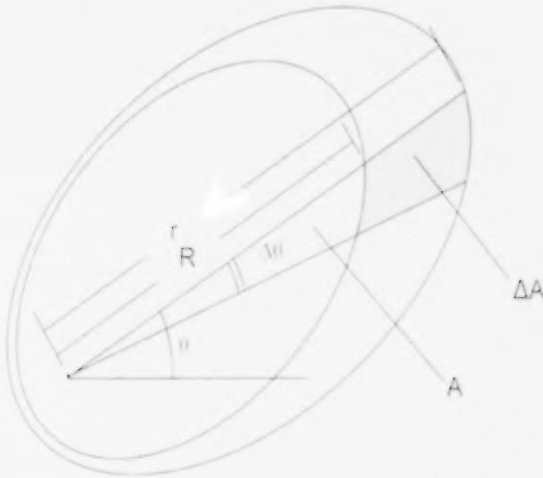
Figure 3. An illustration of the system used to calculate SEI (shaded area), the size difference at angle θ.

If Δθ is small and the unit of angle is in degrees, a and A can be approximated as:

$$a(\theta,t) = \frac{\Delta\theta}{360} \times \left[r^2(\theta,t) \times 2\pi \right] \tag{3}$$

$$A(\theta,t) = \frac{\Delta\theta}{360} \times \left[R^2(\theta,t) \times 2\pi \right] \tag{4}$$

then

$$
\begin{aligned}
SEI(\theta,t) &= a(\theta,t) - A(\theta,t) \\
&= \frac{\Delta\theta}{360} \times \left[r^2(\theta,t) \times 2\pi \right] - \frac{\Delta\theta}{360} \times \left[R^2(\theta,t) \times 2\pi \right] \\
&= \frac{\left[r^2(\theta,t) - R^2(\theta,t) \right] \times \pi \times \Delta\theta}{180}
\end{aligned} \tag{5}
$$

In this study, the perimeters of *actual* fires were represented by the perimeters predicted by the FBP system as discussed above and only the fire perimeters at $t = 15$ h and $\Delta\theta = 0.1°$ were compared. To determine the relative weight of SEI in relation to the actual fire size S, a ratio, T_R, fire size error index, was calculated:

$$
\begin{aligned}
T_R(\theta) &= \frac{SEI(\theta)}{S} \\
&= \frac{\dfrac{\left[r^2(\theta) - R^2(\theta) \right] \times \pi \times 0.1}{180}}{S} \\
&= \frac{\left[r^2(\theta) - R^2(\theta) \right] \times \pi}{1800 \times S}, \quad \theta = 0, 0.1, 0.2, \cdots, 359.9, \quad S > 0
\end{aligned} \tag{6}
$$

Overall simulation error index

SEI can be used to spatially evaluate fire simulation errors. However, measures are also needed to gauge the overall errors of fire simulation compared to actual fire perimeter or any other perimeter (in this report, perimeters predicted by FBP system). Thus, we used the *Shape Deviation Index, SDI*, as an overall simulation error index, to evaluate how much one fire perimeter deviates from another:

$$SDI = \frac{B + C}{S}, \quad S > 0 \tag{7}$$

where if P is the size of the simulated fire and S is the size of the compared fire, then B is the area of P that is outside of S, and C is the area of S that is outside of P, as shown in Figure 4.

The larger the SDI, the larger the area difference is between the two perimeters. If $SDI = 0$, the perimeters are identical (Figure 4d). When SDI is at its maximum value (when $B=P$ and $C=S$), the two perimeters only intersect at the ignition point, as shown in Figure 4e, or do not touch each other at all.
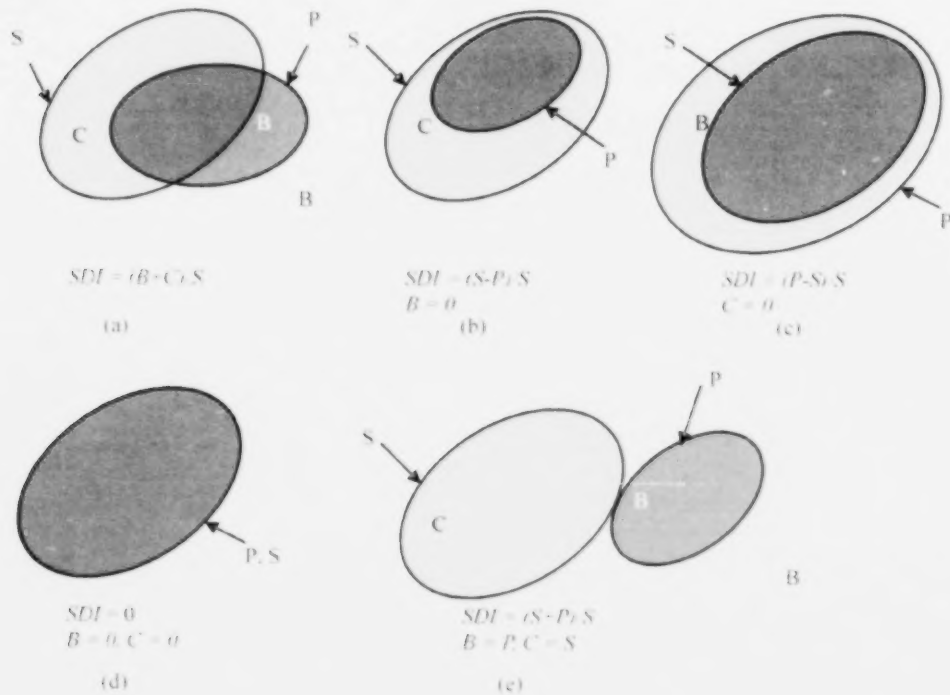
Figure 4. *The five topological relationships between the predicted fire perimeter (P) and the perimeter predicted by the FBP system (S). B is the area of P that is outside of S, and C is the area of S that is outside of P.*

Results

Fire sizes

Fire sizes predicted by the FGMs (hereafter referred to collectively as FGM fire sizes) and fire sizes predicted by the FBP system (referred to as FBP fire sizes) were summarized and compared using ratios, as shown in Figure 5. The ratios were calculated by:

$$Ratio = P / S, \quad S > 0 \tag{8}$$

where P was the FGM fire size and S was the corresponding FBP fire size, which was 11469.53 ha for all wind directions in the uniform fuel type, M1. *Ratio* =1 indicates that the FGM fire size equals the FBP fire size; *ratio* < 1 or > 1 indicates that the FGM fire size is smaller or larger, respectively, than the corresponding FBP fire size.

For the spatial configuration of M1 fuel type (Figure 5, top row), BFOLDS underestimated fire sizes for all four spatial resolutions relative to the FBP system. Fire sizes varied with wind direction with the maximum size at 225° (diagonal). Fire sizes predicted by Prometheus were similar to the corresponding FBP fire sizes for all four spatial resolutions. Wildfire underestimated fire size except for the 4 ha raster size.

For the spatial configuration of RM fuel type, predicted fire sizes (Figure 5, bottom row) differed among the FGMs. BFOLDS consistently overestimated fire size. Its predicted fire sizes varied with wind direction, with maximum sizes predicted for the diagonal direction (225°). Fire sizes were approximately equal for wind directions of 180° and 270° and for wind directions of 202.5° and 247.5°. For
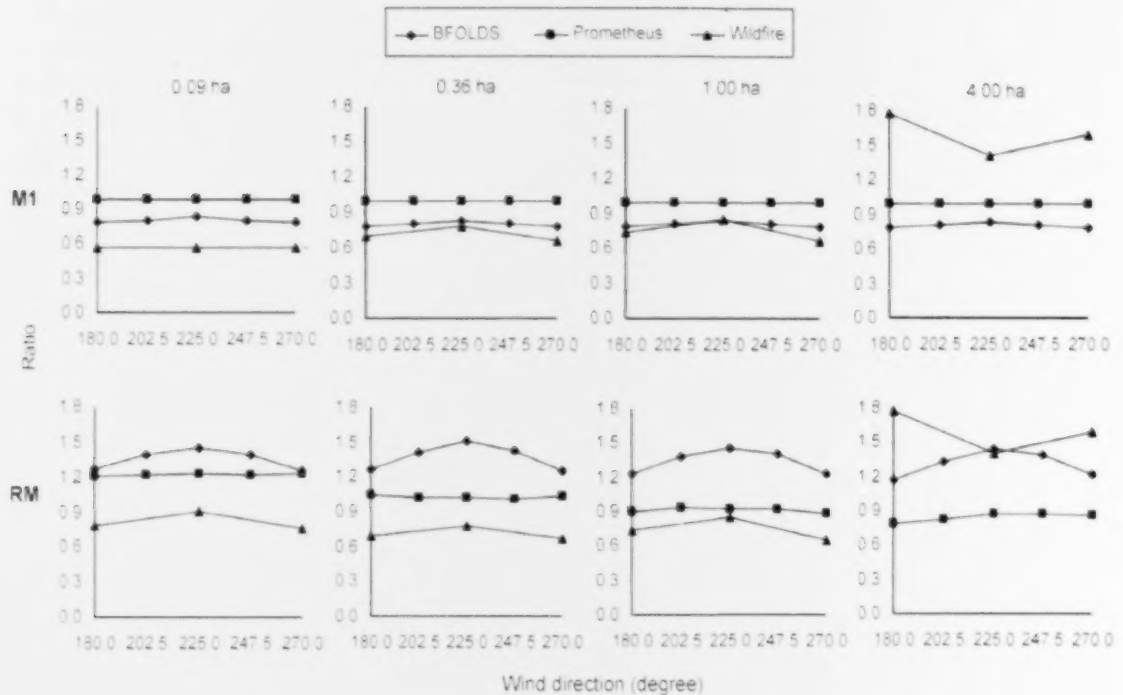
Figure 5. *Ratios of fire sizes predicted by three fire growth models – BFOLDS, Prometheus, and Wildfire – relative to those predicted by the FBP system for various wind directions. The X axis is wind direction in degrees and the Y axis is ratio of fire size. The top row of graphs show results for spatial configurations of M1 fuel type with raster sizes of 0.09, 0.36, 1.00, and 4.00 ha from left to right, respectively; the bottom row shows results for spatial configuration of RM fuel type for the same raster sizes.*

the same wind directions, predicted fire sizes were approximately equal for all four spatial resolutions. Fire sizes predicted by Prometheus varied little with wind direction. However, these fire sizes differed among spatial resolutions: Prometheus overestimated fire sizes by about 20% and 3% of the corresponding FBP fire sizes for raster sizes of 0.09 and 0.36 ha, respectively, and underestimated fire sizes by about 9% and 15% of corresponding FBP fire sizes for raster sizes of 1.00 and 4.00 ha, respectively. Wildfire underestimated fire sizes for raster sizes of 0.09, 0.36, and 1.00 ha, respectively, but overestimated fire sizes for 4.00 ha rasters. Its predicted fire sizes also varied with wind direction: for raster sizes of 0.09 ha, 0.36 ha, and to a certain degree 1.00 ha, fire sizes for wind directions of 180° and 270° were similar and smaller than those for wind direction of 225°; for 4.00 ha raster size, fire sizes for wind directions of 180° and

270° were similar but larger than those for the wind direction of 225°.

Overall fire simulation errors

Similar predicted fire sizes do not necessarily indicate that simulation errors are small, because the larger perimeters do not necessarily completely contain the corresponding small perimeters, as shown in Figures 4a and 4e. A visual illustration of the perimeters for various wind directions and spatial resolutions (Figure 6) provided a lot of information about FGM performance for the three models though it did not help to quantify the simulation errors. We used the overall simulation error index, SDI, to quantify the FGM simulation errors, as summarized in Figures 7 and 8.
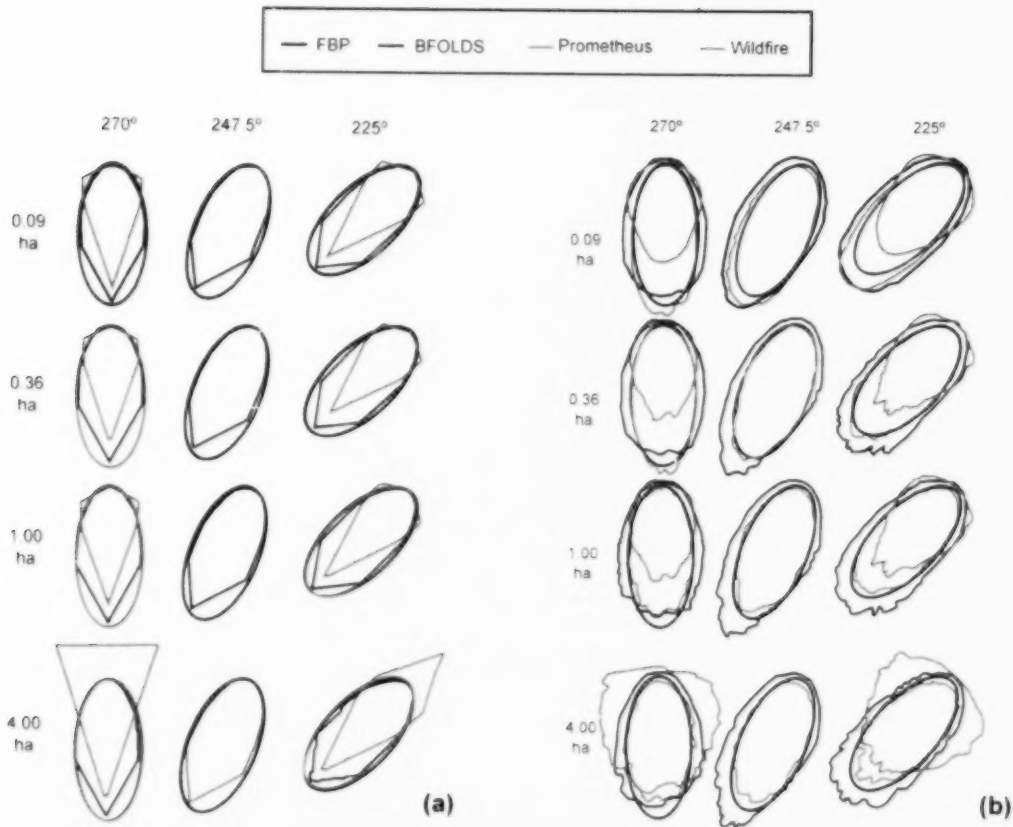
Figure 6. Perimeters predicted by the three fire growth models for various wind directions and spatial resolutions for spatial configurations of fuel types (a) M1 and (b) RM, compared to those predicted by the FBP system. Columns represent wind directions of 270°, 247.5°, and 225° from left to right, for (a) and (b), respectively, and rows represent spatial resolution of raster sizes 0.09, 0.36, 1.00, and 4.00 ha from top to bottom, respectively.

In all cases, the overall simulation errors were smallest for Prometheus and largest for Wildfire. The average *SDI* values for Prometheus, BFOLDS, and Wildfire for all simulations were 0.015, 0.197, and 0.601, respectively, for the spatial configurations of M1 fuel type, and 0.144, 0.386, and 0.609, respectively, for the spatial configuration of RM fuel type.

Spatially explicit fire simulation error analysis

We used the ratio of the fire simulation error index, T_R, to compare FGM-predicted perimeters to FBP-predicted perimeters. Figure 6 shows the perimeters simulated in this study; Figures 8 and 9 show the corresponding ratios (T_R) for the three FGMs for the spatial configurations of M1 and RM fuel type, respectively. Because of the symmetry (M1) or approximate symmetry (RM) of fuel type spatial configurations along the 225° axis, perimeters and corresponding ratio graphs are not shown for wind directions of 202.5° and 180° in the figures because they approximate those at wind directions of 247.5° and 270°.

For the spatial configuration of M1 fuel type, perimeter shapes differed for all three FGMs: BFOLDS perimeters were roughly 16-sided with a pointed angle in the direction of wind; Prometheus perimeters were more elliptical; and Wildfire perimeters were roughly octagonal with a pointed
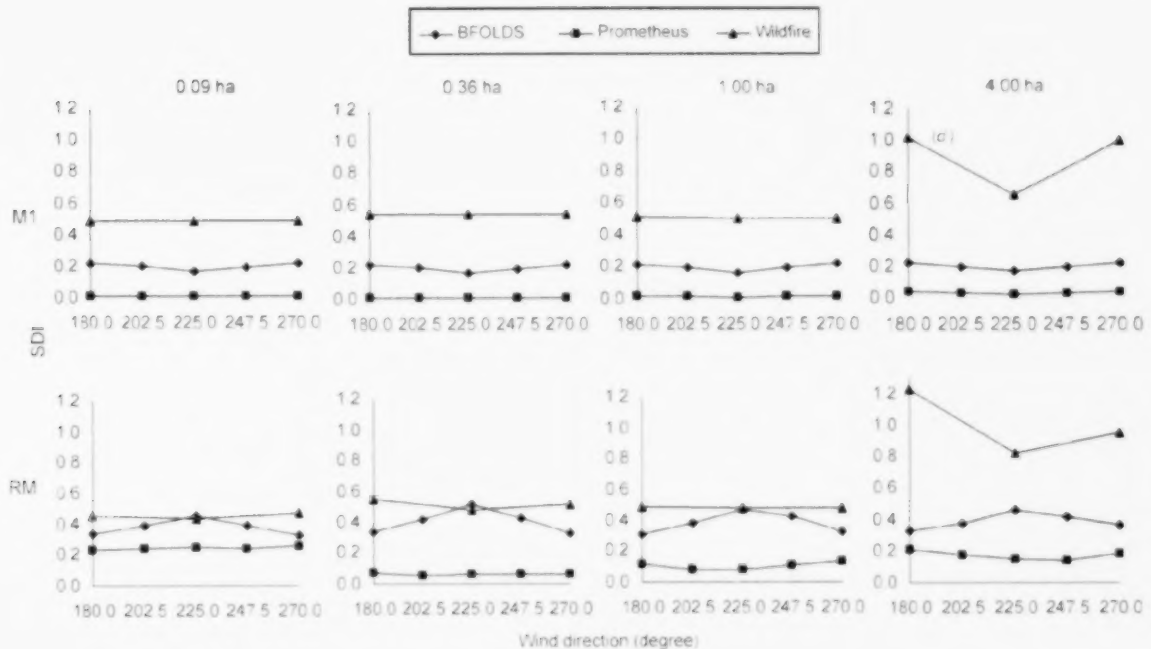
Figure 7. *Overall fire simulation error index, SDI: the top row of graphs show SDI variation with wind direction for the spatial configuration of M1 fuel type with raster sizes of 0.09, 0.36, 1.00, and 4.00 ha, respectively; the bottom row shows the same information for the spatial configuration of RM fuel type.*

angle in the direction of wind (Figure 6a). The perimeters predicted by BFOLDS and Prometheus were within the corresponding FBP perimeters, illustrating why both models underestimated fire sizes for the spatial configuration of M1 fuel type. Although Wildfire also underestimated fire sizes for this fuel type spatial configuration, its predicted perimeters were not completely contained by the corresponding FBP perimeters: parts of fire flanks fell outside. For Wildfire the most important result was that both the shape and area of its predicted perimeters at the 4 ha raster size differed from those at smaller raster sizes (0.09, 0.36, and 1.00 ha).

For the spatial configuration of RM fuel type, predicted fire perimeter shapes also differed among FGMs, but were all somewhat elliptical (Figure 6b). Perimeters predicted by BFOLDS differed among wind directions but were similar in shape for all spatial resolutions. At 270° and 180° wind directions,

perimeters fell outside the corresponding FBP perimeters except in the head fire directions (decided by the wind directions in this study). Perimeters were outside the corresponding FBP perimeters for all other wind directions tested.

The fire size error index graphs (Figures 8 and 9) show the magnitude of the simulation errors by fire spread direction. Although errors were evident for all fire growth directions, fire growth simulation errors were largest for an angle range of roughly 150° around the direction of wind (i.e., +/- 75° of the wind direction), except for the perimeters predicted by Wildfire at the raster size of 4 ha.

Also, for the wind directions of 202.5° and 247.5°, perimeter shapes of the two raster-based FGMs shifted towards the diagonal axis, which is 225° as shown visually in Figure 6 and quantitatively in Figures 8 and 9 using the fire size error index (T_R).

Figure 8. Graphs of the fire size error index (T_R) for the spatial configuration of M1 fuel type for three FGMs. Graphs within columns are for wind directions of 270°, 247.5°, and 225°, from left to right. Graphs within rows are for spatial resolutions of raster sizes 0.09, 0.36, 1.00, and 4.00 ha, from top to bottom. On each graph, the X axis is fire spread direction and the Y axis is fire size error index, T_R.
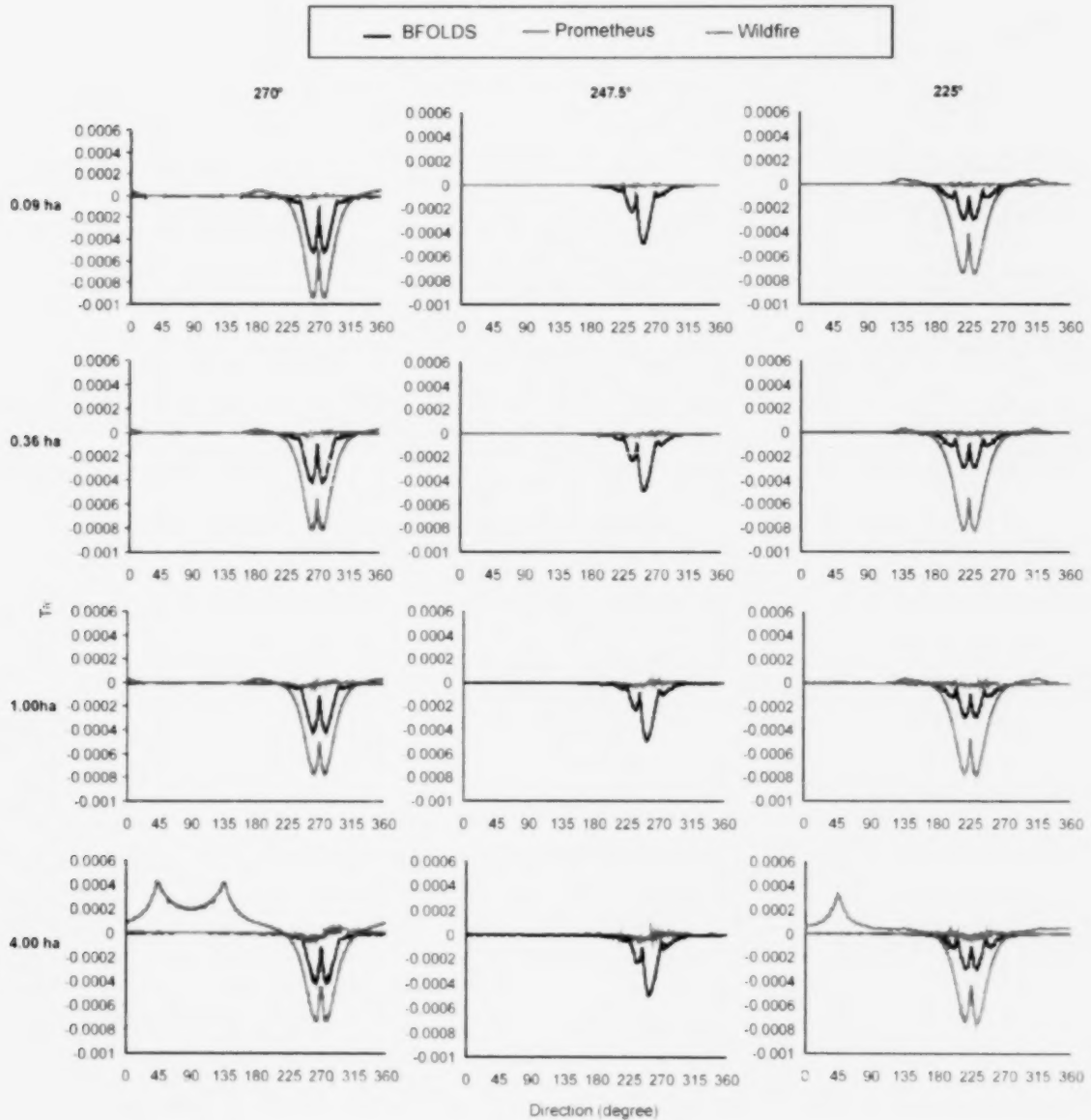
Figure 9. Graphs of the fire size error index (T_{si}) for the spatial configuration of RM fuel type for three FGMs. Graphs within columns are for wind directions of 270°, 247.5°, and 225°, from left to right. Graphs within rows are for spatial resolutions of raster sizes 0.09, 0.36, 1.00, and 4.00 ha, from top to bottom. On each graph, the X axis is fire spread direction and the Y axis is fire size error index, T_{si}.
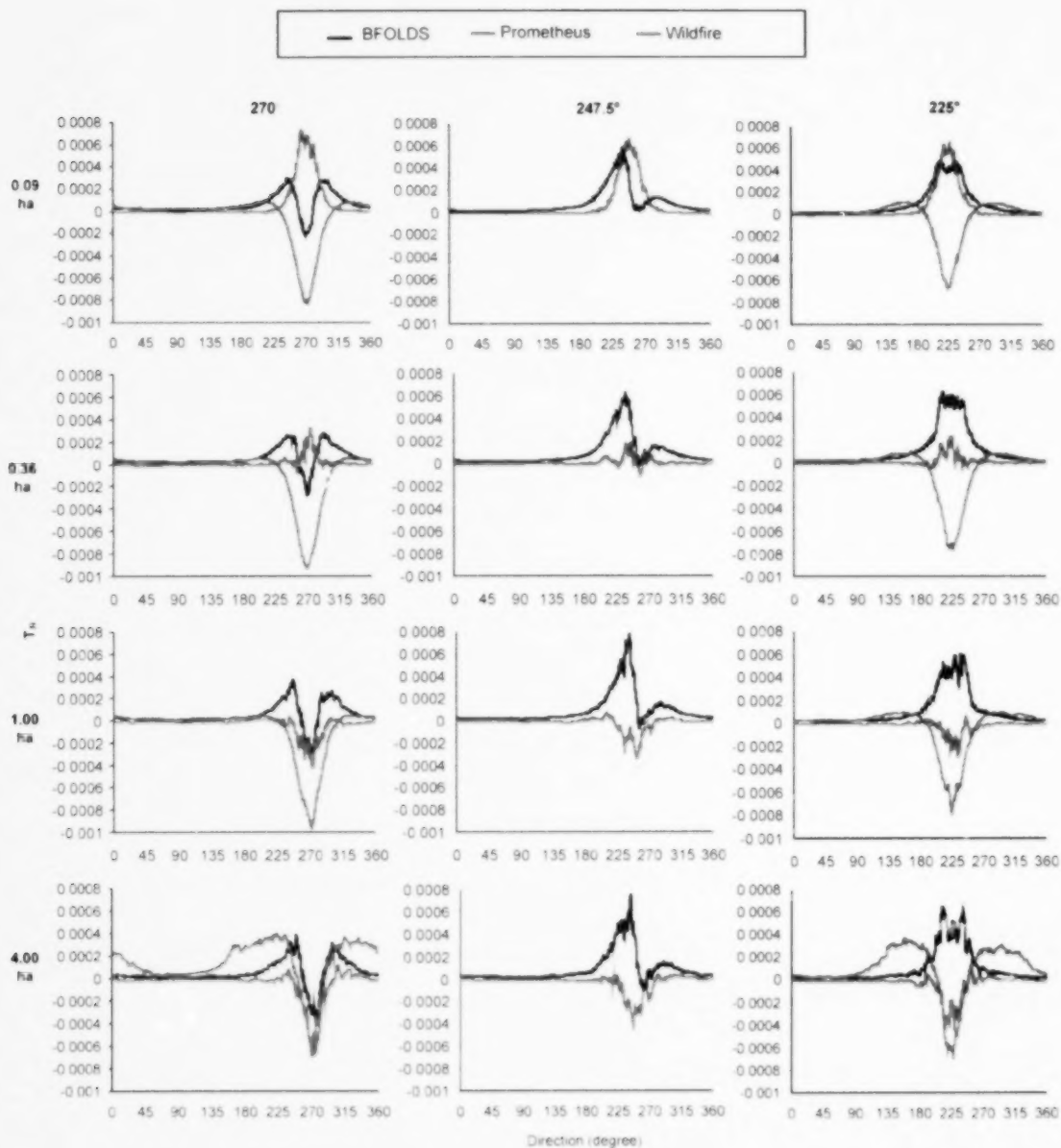
Discussion

Simulation error analysis

Since we used the same input data and fire behaviour model, the Canadian FBP system, and compared results to theoretical predictions of the FBP system, we could attribute all the simulation errors to the fire growth algorithms in the three models we compared. For the two raster-based models, some of the simulation errors were caused by shape distortion of the fire perimeters because of their limited number of regular fire growth directions (Feunekes 1991, French 1992, Finney 2004, Trunfio 2004). Specifically, Wildfire has only eight spread directions while BFOLDS has 16, which cause these to produce octagonal and 16-sided polygon perimeters, respectively, in uniform fuel and topography under constant weather conditions. Even without simulation error in the eight or 16 directions, the raster-based FGMs would underestimate fire size, and the octagon more so than the 16-sided polygon.

The shape distortion of the two raster-based FGMs was reduced in the spatial configuration of RM fuel type: all the perimeters looked roughly elliptical. However, the overall simulation errors, as shown by the average SDIs, were larger than those in the M1 configuration for all three FGMs (Figures 6, 8, and 9). This suggests that shape distortion was masked by the heterogeneous fuel configuration but the simulation errors caused by shape distortion still existed and were even larger. For the raster-based FGMs, it is likely that the shape distortion could be further masked in more heterogeneous landscapes and changing weather conditions.

For Prometheus and Wildfire, simulation errors could also result from the way they advance time: they grow fires by discrete time steps and only calculate and project the fire perimeters at each time step. Then, based on the new perimeter, they project a perimeter for the next time step. For each time step, simulation errors occur because the perimeters are polygons rather than the theoretical ellipse: even for Prometheus with its vector-based algorithm that allows it to spread in small time steps within a raster. For Wildfire, the minimum fire growth distance is the width of one raster. Thus, the simulation errors were even larger for each time step.

BFOLDS advances time continuously based on an event-driven algorithm. This event-driven algorithm avoids the accumulated simulation errors caused by discrete time steps. It also enables the simultaneous simulation of multiple fires on a landscape of tens of millions of hectares over the whole fire season.

Wildfire simulation error increased considerably at the 4 ha resolution. This behaviour might be due to a simple coding error or a violation of Courant-Friedrichs-Lewy (CFL) condition (Courant et al. 1967) in its algorithm when using coarser spatial resolutions (4 ha or larger raster size), where it must meet the following condition:

$$r \cdot \Delta t \gg \Delta x \tag{9}$$

where r is the rate of spread, Δt is the time step, and Δx is the cross-sectional width of a cell.

Simulation errors were highest for an angle range of fire spread direction of roughly 150° around the direction of wind because the ROS in those directions are larger, thus so were the errors in the spread distance. However, even if simulation errors in distance were similar in all directions, the simulation errors in size were much larger in the direction of wind, as expressed in equation 5.

Effect of wind direction

While Prometheus predictions did not vary much with wind direction, the fire sizes, simulation errors, and shapes predicted by BFOLDS and Wildfire varied as shown in Figures 5, 6, 8, and 9. For the spatial configuration of M1 fuel type, fire sizes predicted by BFOLDS varied among wind directions with the biggest difference at 225° (diagonally across the landscape); those predicted by Wildfire varied the most overall. For the spatial configuration of RM fuel type, fire sizes predicted by the two raster-based FGMs (BFOLDS and Wildfire) varied even more with wind direction though trends were similar, especially for BFOLDS.

As discussed in the simulation error analysis section, the sensitivity of BFOLDS and Wildfire to wind direction was caused by the shape distortion of the fire perimeters resulting from the limited number of regular fire spread directions, an inherent problem for raster-based models (Feunekes 1991, French 1992, Finney 2004, Trunfio 2004).

Since the wind direction here happens to be the direction of maximum speed of fire spread (head fire spread direction), which can also be affected by slope and aspect if slope is not zero, the effect of wind direction can be generalized as that of head fire spread direction.

The algorithm sensitivity to wind direction has implications for applying the FGMs in both research and operations. Even when all the other parameters, such as ignition location, fuel, and weather conditions are constant, the FGMs might predict fire size and perimeter differently, especially the two raster-based models.

Effect of spatial resolution

The relationships between FGM fire sizes, shapes, and simulation errors and the spatial resolution of input are shown in Figures 10 and 11. BFOLDS and Prometheus fire sizes and shapes overall did not vary widely with spatial resolutions for the spatial configuration of M1 fuel type. BFOLDS fire sizes and shapes varied very little for the spatial configuration of RM fuel type while those predicted by Prometheus decreased with decreasing spatial resolutions (increasing raster size). However, the most accurate prediction (compared to those from the FBP system) did not occur at the highest resolution. This suggests that the prediction accuracy cannot be improved just by increasing the spatial resolution: there is not an optimum spatial resolution for each simulation scenario. The relationship between the fire sizes predicted by Wildfire and spatial resolution was not consistent: fire sizes were smallest at 0.36 ha raster size. Also, the shapes and areas of predicted perimeters at the 4 ha raster size differed from those at smaller raster sizes (0.09, 0.36, and 1.00 ha) and thus larger simulation errors occurred in almost all spread directions. This suggests that caution is needed when Wildfire is used with spatial inputs of raster sizes of 4 ha or larger.
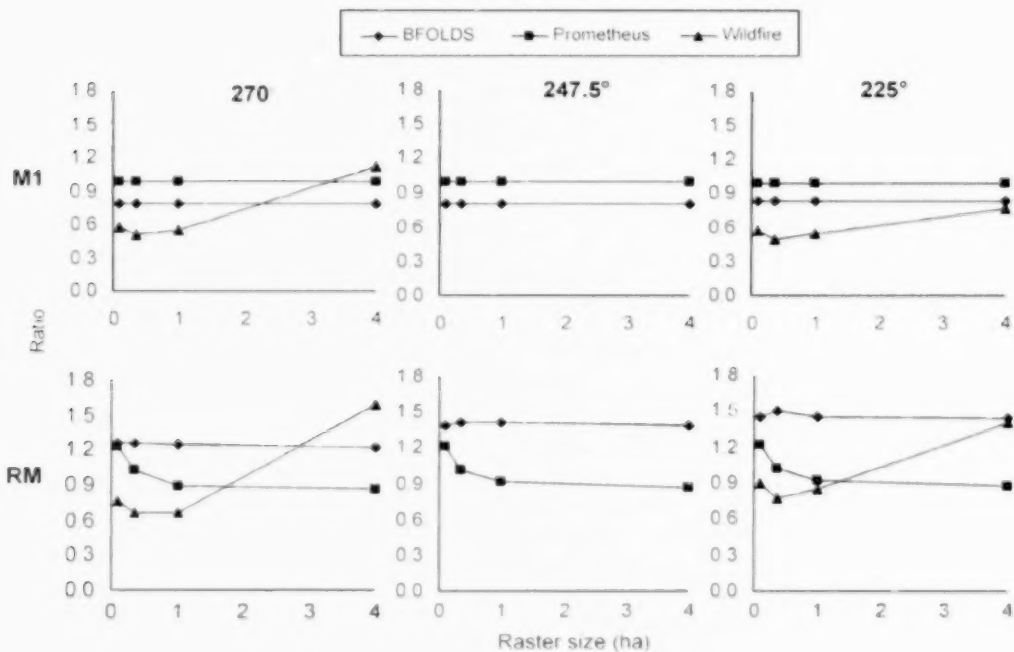
Figure 10. Ratios of fire sizes predicted by three fire growth models to those predicted by the FBP system for different spatial resolutions (defined by raster sizes). The X axis is raster size in ha and the Y axis is ratio of fire size. The top row of graphs show results for spatial configurations of M1 fuel type for wind directions of 270°, 247.5°, and 225° from left to right, respectively; the bottom row of graphs show results for spatial configuration of RM fuel type also for wind directions of 270°, 247.5°, and 225°, respectively.

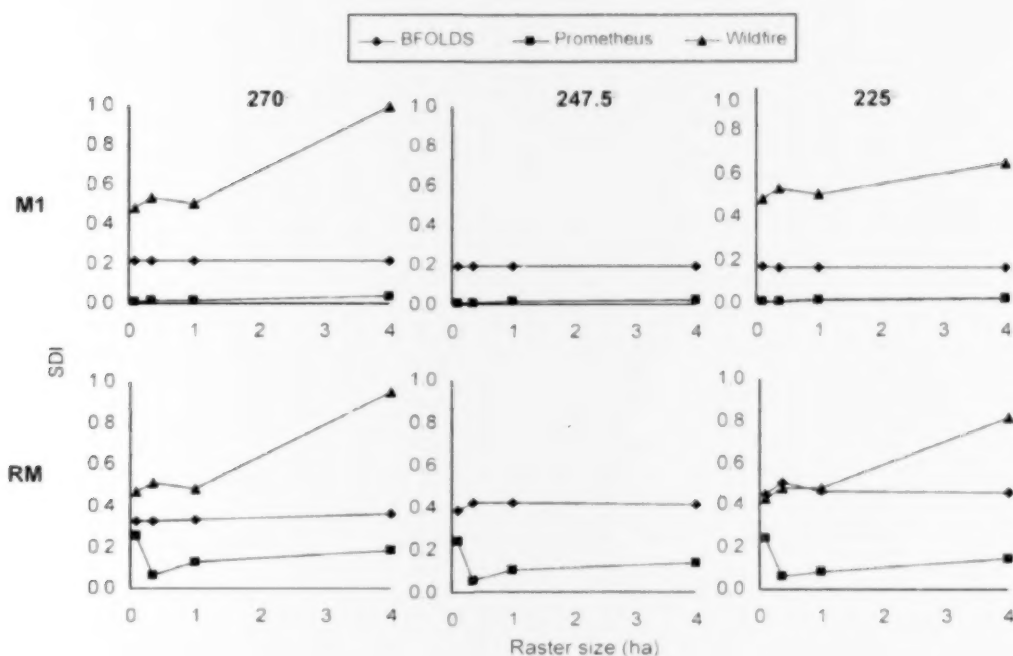**Figure 11.** Graphs of overall fire simulation error index (SDI). The X axis is raster size in ha and the Y axis is overall simulation error index, SDI. The top row of graphs show results for spatial configurations of M1 fuel type for wind directions of 270°, 247.5°, and 225°, respectively; the bottom row of graphs show results for spatial configuration of RM fuel type also for raster wind directions of 270°, 247.5°, and 225°, respectively.

The overall fire simulation errors for BFOLDS and Prometheus remained constant over the four spatial resolutions for the spatial configuration of M1 fuel type while those for Wildfire increased with increasing raster sizes. For the spatial configuration of RM fuel type, simulation errors for both Prometheus and Wildfire increased with increasing raster size while those of BFOLDS varied little.

That BFOLDS predictions varied little or not at all for different spatial resolutions might be explained by its use of an event-driven time advancing algorithm that avoids accumulated errors caused by discrete time steps. This also suggests that Prometheus and Wildfire were sensitive to spatial resolutions because they advance time discretely, and thus introduce simulation errors at each time step.

Model improvement

The sensitivity of BFOLDS and Wildfire predictions to wind directions cannot be significantly minimized by increasing the spatial resolution of the input data. This is because errors are caused by the shape distortion due to the fixed number of regular pathways for fire travel (Finney 2004) and the raster's square shape (Feunekes 1991, French 1992, Trunfio 2004), which means fire travel distances differ from source raster to neighbouring rasters, as shown in Figure 2. To improve on the first problem, more fire spread directions could be added. To address the second problem, raster shape may need to be changed, for example, to a hexagon (Trunfio 2004).

From the fire size error index graphs (Figures 8 and 9), the majority of fire size error was in the direction of head fire, roughly in a range of 150°. Thus, fire growth modelling improvements should concentrate on

improving the head fire growth algorithm (Feunekes 1991). For vector-based models, such as Prometheus, this might mean increasing the density and number of fire vertices in the direction of fire head. For raster-based FGMs, it might be better to add more spread directions in the fire head rather than adding spread directions over the whole 360° range as per tradition. Although this would increase the complexity of the algorithm, it greatly reduces simulation time (Feunekes 1991).

Apart from increasing fire spread directions, another algorithm change might greatly enhance the performance of BFOLDS. That is, using all the fuel types between the target raster and the source raster to calculate ROS. The present version of BFOLDS only uses the fuel type of the source raster to calculate the ROS for each spread direction, regardless of the fuel types of neighbouring rasters (Figure 2). This explains why BFOLDS overestimated fire sizes for the spatial configuration of RM fuel type: BFOLDS spreads fires in unburnable directions. For example, the ROS to raster 10 is based on ROS of the fuel type in the source raster but it should be 0 because raster 11, which is on the spread path, is unburnable (Figure 2). Also BFOLDS overestimates average ROS to the target raster if the fuel type in the source raster is C2 (in which ROS is much higher) and D1 fuel type rasters (in which ROS is much lower) are in the path to the target raster or in the target raster itself. For example, for fire to spread from the source raster with fuel type C2 to target raster 14, the average ROS is greatly overestimated because it does not account for the lower ROS in rasters 9 and 14, in which the fuel type is D1 (Figure 2). On the other hand, there is a smaller possibility and/or degree of underestimating ROS if the fuel type in the source raster is D1 because the target rasters are more likely to have been burned by fires spread from nearby source rasters whose fuel types are C2.

Interactions among three sources of simulation errors and future research directions

As evident from our study results, significant simulation errors can arise from the algorithm of FGMs: the average SDIs were 0.015, 0.197, and 0.601 for Prometheus, BFOLDS, and Wildfire, respectively,

for the spatial configurations of M1 fuel type and 0.144, 0.386, and 0.609, respectively, for the spatial configurations of RM fuel type. This error that resulted from fire growth algorithm is only one of three sources of fire growth modelling errors as shown in Figure 1. We know little about how the three source of error interact, though we have limited knowledge of how weather data quality might affect simulation error (Anderson at el. 2007) and how the fire growth algorithm can contribute to simulation error as shown in this study. However, simulation error might accumulate in the sequence shown in Figure 1. The error originates from input data, then propagates through the imperfect fire behaviour model, and the final simulation error is decided by the fire spread algorithm of the FGM. The magnitude of final overall simulation error can change in three ways: become larger, be identical (almost impossible), or be smaller. However, from a spatio-temporal perspective, an almost infinite number of combinations are possible: the error may increase or decrease in one direction at a certain time but may do otherwise at another time. That is, some errors may compensate for other errors. It is also difficult to say which source of error will dominate depending on the quality of input data and specific fire modelling conditions, such as weather, wind direction, and spatial configuration of fuel types. All these aspects deserve further investigation.

In addition, better understanding of these sources of errors and their interactions might reveal the directions for improving fire growth algorithms and even forest fire behaviour models. This study covers only one of the three sources of simulation errors of FGMs and only three factors that affect fire growth algorithms. Further studies on the other two sources of error are needed, and the effects of more factors, such as weather variables and topography, on simulation errors from fire growth algorithms should be studied. For each variable, more levels of values, such as more spatial configurations of fuel types, should be included in these investigations.

Thorough understanding of these sources of simulation errors, both separately and collectively their interactions, might help model users to understand the limitations and advantages of FGMs and adopt measures to reduce the final simulation errors. This will improve the usefulness of FGMs for both research and operations.

Summary and Conclusions

Algorithm-caused errors

Fire growth algorithms caused simulation errors in all three FGMs under all the conditions we studied. Specifically: (1) the fire growth simulation errors occurred mainly in the direction of fire head within a relatively narrow range; (2) finer spatial resolutions of input data do not necessarily produce more accurate predictions for all three FGMs; (3) the FGM predictions varied greatly with fuel type spatial configuration even though the fuel type compositions were identical; and (4) the event-driven continuous time advancing algorithm helps to reduce error accumulation.

The characteristics and relative magnitude of errors varied among the three FGMs: (1) Fire size and shape errors associated with the algorithm in the BFOLDS model were influenced by wind direction but varied little with spatial resolution. (2) Prometheus simulations contained small algorithm errors under uniform fuel and topography configurations and constant weather conditions, but fire sizes and shapes varied with spatial resolution in the randomly mixed fuel types. (3) Wildfire was sensitive to both wind direction and spatial resolution.

Causes of errors

The overall fire simulation error index, SDI, was effective in quantifying the overall fire spread simulation errors, especially for comparison purposes. The fire simulation error index, SEI, helped to spatially explicitly quantify the simulation error by spread direction. We found: (1) Some of the simulation errors of the two raster-based models (BFOLDS and Wildfire) were caused by the shape distortion of the fire perimeters resulting from limited number of regular fire spread directions and the square shape of the rasters. (2) The use of discrete time steps to project fire perimeters might result in greater error accumulation than the event-driven continuous time advancing algorithm. (3) The use of discrete time steps to project fire perimeters might cause a violation of Courant-Friedrichs-Lewy (CFL) condition (Courant et al. 1967), which greatly increases simulation error.

Algorithm improvement

Better understanding of these sources of simulation errors, both separately and collectively for their interactions, might facilitate further improvement of fire growth algorithms and improve use of FGMs in research and operations. In this study, we identified some directions for improvement for all FGMs: (1) For vector-based models, this might mean increasing the density and number of fire vertices in the direction of fire head. For raster-based FGMs, it might be better to add more spread directions in the fire head rather than adding spread directions over the whole 360° range as per tradition. 2) For raster-based FGMs, using all the fuel types between the target raster and the source raster to calculate ROS would improve their predictions. This is not a limitation for vector-based FGMs.

Future research directions

To further improve FGMs, investigations are needed to (1) explore the effects of the other two sources of simulation errors of FGMs, (2) evaluate additional factors, such as various weather variables and topography, (3) for each variable, include more levels of values, such as more spatial configurations of fuel types, and (4) more importantly, assess the interactions among these sources of errors.

References

Anderson, K., G. Reuter, M.D. Flannigan. 2007. Fire-growth modelling using meteorological data with random and systematic perturbations. International Journal of Wildland Fire 16: 174-182.

Berjak, S.G. and J.W. Hearne. 2002. An improved cellular automaton model for simulating fire in a spatially heterogeneous Savanna system. Ecological Modelling 148: 133-151.

Catchpole, E.A., N.J. de Mestre and A.M. Gill 1982. Intensity of a fire at its perimeter. Australian Forestry Research 12: 47-54.

Courant, R., K. Friedrichs and H. Lewy. 1967. On the partial difference equations of mathematical physics. IBM Journal March 1967: 215-234. (English translation of the 1928 German original.)

CWFGM Project Steering Committee. 2006. Prometheus user manual Version 4.3. http://www.firegrowthmodel.com/download/PrometheusVer_4.3UserManual.pdf (Accessed February 6, 2007).

Feunekes, U. 1991. Error analysis in fire simulation models. MS Thesis, University of New Brunswick. Fredericton, NB.

Finney, M.A. 2001. Design of regular landscape fuel treatment patterns for modifying fire growth and behaviour. Forest Science 47: 219-228.

Finney, M.A. 2004. FARSITE: Fire area simulator—Model development and evaluation. USDA Forest Service, Rocky Mountain Research Station, Ogden, UT. Research Paper RMRS-RP-4 (Revised).

Forestry Canada Fire Danger Group. 1992. Development and structure of the Canadian Forest Fire Behavior Prediction System. Forestry Canada, Science and Sustainable Development Directorate, Ottawa, ON. Information Report ST-X-3.

French, I.A. 1992. Visualisation techniques for the computer simulation of bushfires in two dimensions. MS Thesis, University of New South Wales. Sydney, NSW.

Fujioka, F.M. 2002. A new method for the analysis of fire spread modeling errors. International Journal of Wildland Fire 11: 193-203.

Hargrove, W.W., R.H. Gardner, M.G. Turner, W.H. Romme and D.G. Despain. 2000. Simulating fire patterns in heterogeneous landscapes. Ecological Modelling 135: 243-263.

Opperman, T., J. Gould, M. Finney and C. Tymstra. 2006. Applying fire spread simulators in New Zealand and Australia: Results from an international seminar. Pp. 201-212 in P.L. Andrews and B.W. Butler, eds. Fuels Management—How to Measure Success. USDA Forest Service, Rocky Mountain Research Station, Fort Collins, CO. Proceedings RMRS-P-41.

Perera, A.H., D.J.B. Baldwin, D.G. Yemshanov, F. Schnekenburger, K. Weaver and D. Boychuk. 2003. Predicting the potential for old growth forests by spatial simulation of landscape aging patterns. Forestry Chronicle 79: 621-631.

Perera, A.H., D. Yemshanov, F. Schnekenburger, D.J.B. Baldwin, D. Boychuk and K. Weaver. 2004. Spatial simulation of broad-scale fire regimes as a tool for emulating natural forest landscape disturbance. Pp. 112-122 in A.H. Perera, L.J. Buse and M.G. Weber, eds. Emulating Natural Forest Landscape Disturbances: Concepts and Applications. Columbia University Press, New York, NY.

Richards, G.D. 1990. An elliptic growth-model of forest-fire fronts and its numerical-solution. International Journal for Numerical Methods in Engineering 30: 1163-1179.

Richards, G.D. and R.W. Bryce. 1995. A computer algorithm for simulating the spread of wildland fire perimeters for heterogeneous fuel and meteorological conditions. International Journal Wildland Fire 5: 73-79.

Rothermel, R.C. 1972. A mathematical model for predicting fire spread in wildland fuels. USDA Forest Service, Intermountain Research Station, Ogden, UT. Research Paper INT-115.

Sánchez-Guisández, M., W. Cui and D.L. Martell. 2002. FireSmart strategies for wildland urban interface landscapes. Pp. 121-130 in Proceedings, IV International Conference on Forest Fire Research, Luso, Coimbra, Portugal. Millpress, Rotterdam.

Sánchez-Guisández, M., W. Cui and D.L. Martell. 2007. A decision support system for evaluating fuel management strategies for wildland urban interface areas. In Proceedings, IV International Wildland Fire Conference. Seville, Spain.

Todd, B. 1999. User documentation for the Wildland Fire Growth Model and the Wildfire Display Program. Canadian Forest Service. Edmonton, AB. Unpublished Report.

Trunfio G.A. 2004. Predicting wildfire spreading through a hexagonal cellular automata model. Pp. 385-394 in Sloot, P.M.A., B. Chopard and A.G. Hoekstra, eds. Cellular Automata. Springer-Verlag, Berlin, Germany.

Van Wagner, C.E. and T.L. Pickett. 1985. Equations and FORTRAN program for the Canadian Forest Fire Weather Index System. Canadian Forest Service, Ottawa, ON. Forestry Technical Report 33.